Wind and Structures, Vol. 4, No. 1 (2001) 1-18
DOI: http://dx.doi.org/10.12989/was.2001.4.1.001

A deformable section model for the dynamics of suspension bridges. Part I : Model and linear response

Vincenzo Sepe† and Giuliano Augusti‡

Dipartimento di Ingegneria Strutturale e Geotecnica, Università di Roma "La Sapienza" , via Eudossiana 18, 00184 Roma, Italy

Abstract. The classical two-degree-of-freedom (2-d-o-f) "sectional model" is currently used to study the dynamics of suspension bridges. Taking into account the first pair of vertical and torsional modes of the bridge, it describes well *global* oscillations caused by wind actions on the deck and yields very useful information on the overall behaviour and the aerodynamic and aeroelastic response, but does not consider *relative* oscillation between main cables and deck. The possibility of taking into account these relative oscillations, that can become significant for very long span bridges, is the main purpose of the 4-d-o-f model, proposed by the Authors in previous papers and fully developed here. Longitudinal deformability of the hangers (assumed linear elastic in tension and unable to react in compression) and external loading on the cables are taken into account: thus not only *global* oscillations, but also *relative* oscillations between cables and deck can be described. When the hangers go slack, large nonlinear oscillations are possible; if the hangers remain taut, the oscillations are small and essentially linear. This paper describes the model proposed for small and large oscillations, and investigates in detail the limit condition for linear response under harmonic actions on the cables (e.g., like those that could be generated by vortex shedding). These results are sufficient to state that, with geometric and mechanical parameters in a range corresponding to realistic cases of large span suspension bridges, large relative oscillations between main cables and deck cannot be excluded, and therefore should not be neglected in the design. Forthcoming papers will investigate more general cases of loading and dynamic response of the model.

Key words: suspension bridges; wind effects; sectional model; nonlinear dynamics; vortex shedding.

1. Introduction

The design of long span suspension bridges under wind action is usually performed by means of mechanical models and then carefully assessed through wind tunnel tests on rigid section or scaled models of the whole bridge. Both very complex or very simplified numerical and experimental models are used in current practice. Examples of the first are sophisticated finite element models, which can take into account appropriate wind time-histories and also structural details; however, the interpretation of their results can be difficult, because of the very large number of degrees of freedom involved and of the many input data required to define properly the wind action along the span. On the contrary, the results given by simplified models can be interpreted more easily and are

† Assistant Professor
‡ Professor

therefore convenient at least at a preliminary design stage; however, they may miss aspects that can become very significant in particular situations. For example, the classical 2-d-o-f "sectional model", widely used also in experimental investigations, allows to consider only two natural modes related to *global* oscillations of the bridge, while neglecting the direct loading on the cables, the longitudinal deformability of the hangers and their lack of compression resistance. This model, therefore, can yield very useful information on the overall behaviour and the aerodynamic and aeroelastic response, but cannot describe any *relative* oscillations between main cables and deck that, as recently shown (Augusti *et al.* 1997, Augusti and Sepe 1999) can be significant and potentially dangerous for very long span bridges and wind velocities within realistic limits.

To the authors' knowledge, the first authors who tackled the effects of the unilateral behaviour of hangers (elastic in tension but without any strength in compression) and of the direct loading on the cables were McKenna and his co-workers (McKenna and Walter 1987, Glover *et al*. 1989, Lazer and McKenna 1990). In particular, they attribute to the unilateral behaviour of hangers some peculiar and unusual aspects of the response of the Tacoma Narrows bridge well before collapse conditions, like large amplitude vertical oscillations under relatively low wind speed (Glover *et al.* 1989). The unilateral behaviour of hangers, according to Lazer and McKenna (1990) is also responsible for the travelling waves observed on the Golden Gate bridge (USA) during an unusually violent storm (February 1938) and the seismic oscillations of the same bridge during the California earthquake of 1989 (≪ According to witnesses ... the bridge did indeed go immediately into the nonlinear regime, with the stays connecting the roadbed to the cables alternately loosening and tightening "like spaghetti" ≫, Lazer and McKenna 1990).

In their 1987 paper, McKenna and Walter studied the response of a one-dimensional beam (representing the deck) suspended by unilateral elastic hangers to the main cables, considered as fixed constraint; the possibility of both small (linear) and large amplitude vertical oscillations was shown under the action of the deck weight and of a periodic forcing with appropriate intensity and frequency. Glover *et al*. (1989), considering only vertical oscillations without nodes, reduced the previous beam model to a one-degree-of-freedom model, however sufficient to explain the already recalled large amplitude oscillations of the Tacoma Narrows bridge. Later, this model was extended into two 2-d-o-f models (Lazer and McKenna 1990) that take into account respectively (*i*) the vertical displacements of the cables (assumed equal to each other) and of the deck, and (*ii*) the vertical displacement and torsional rotation of the deck, allowed by the differential deformation of the hangers, without displacement of the main cables. In both models the hangers are modelled as linear elastic in tension and unable to react in compression.

These papers have been reconsidered by Doole and Hogan (1996) who have investigated linear and nonlinear response of the 1-d-o-f model of Glover and co-workers under harmonic forcing and discussed the stability of periodic response: some results of this paper will be examined later (Section 5). Recently, Ahmed and Harbi (1998) have presented a mathematical analysis of the continuous model of Lazer and McKenna (1990) and discussed linear and nonlinear oscillations, either free or under moving loads, in presence of aerodynamic damping; the energy transfer between cables and deck has also been shown for several examples.

The four-degree-of-freedom "*deformable section*" model, already proposed by the writers (Augusti *et al.* 1997, Augusti and Sepe 1999), combines and extends McKenna's numerical models by considering at the same time torsional rotation and vertical displacement of the deck and vertical displacements of the two cables (Fig. 1). As in the quoted papers by McKenna and co-workers, the hangers are assumed linear elastic in tension and ineffective in compression: thus, the proposed model, further

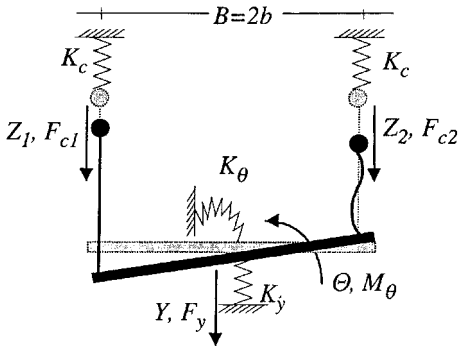

Fig. 1 The 4-d-o-f "*deformable section*" model

developed in this paper, is able to describe the global and relative oscillations for the whole range of behaviour of the hangers; to the authors' knowledge, no analytical sectional model had ever been related to these relative oscillations before. In fact, even very recent investigations on the condition for incipient multi-modal dynamic instability, that can become relevant for long bridges (Jain *et al.* 1996, D'Asdia and Sepe 1998) keep assuming a rigid behaviour of the cross-section. On the contrary, the theoretical and numerical analyses developed in this paper and in its follow-up (Sepe and Augusti 2001) confirm the already presented preliminary results (Augusti *et al*. 1997, Augusti and Sepe 1999), i.e., that, in the case of very large bridges, significant relative motions can develop because of the zero stiffness of the hangers when in compression.

The full behaviour of the proposed model can be found only by step-by-step integration of the equations of motion, because of the discontinuity and the consequent nonlinearity of the equations of motion. It has deemed therefore appropriate to examine first in full detail the conditions that guarantee small amplitude oscillations (hangers always taut) around the equilibrium configuration, and exclude large amplitude oscillations (hangers loosening and tightening, alternatively). As described in Section 4.2 and Section 4.3, this analysis shows that the possibility of the latter type of response may arise under wind speeds within realistic limits.

The forthcoming Part II (Sepe and Augusti 2001) will investigate and discuss the nonlinear dynamic behaviour of the model for wind-induced forces both on the main cables and on the deck.

2. The proposed model

The proposed analytical model aims at describing the oscillations of a suspension bridge induced by fluctuating actions on the main cables and on the deck around the configuration of equilibrium under dead loads.

While cables and deck are assumed to behave elastically, hangers are considered as linear elastic in tension and ineffective in compression; because of pre-tension due to deck weight in the reference configuration, this unilateral behaviour becomes significant depending on the amplitude of the relative oscillations.

In order to obtain still a relatively simple model, however, it is assumed that the three principal components of the bridge, namely the main cables and the deck, oscillate with the same longitudinal shape $\psi(x)$, although not with the same amplitudes. This is indeed the assumption under which all sections behave in a similar way, and therefore the bridge response can be described by a "sectional

model": in the present case, a "deformable section" model, that improves the classical 2-d-o-f rigid-section model, because it is able to account for relative displacements between main cables and deck, made possible by the elasticity of the hangers in tension and their "slackness" in compression.

Let x and t be the coordinate along the bridge axis and the time, respectively, and assume the same shape $\psi(x)$ for the first vertical and torsional modes of oscillation of the bridge deck: the vertical displacement $y(x, t)$ and the rotation $\theta(x, t)$ of any generic cross section of the deck can be written:

$$y(x, t) = Y(t)\ \psi(x)\ ; \qquad \theta(x, t) = \Theta(t)\psi(x) \tag{1}$$

where $x \in [0, L]$, with L the length of the main span of the bridge, and $Y(t)$ and $\Theta(t)$ are the generalised displacement or rotation related to the assumed pseudo-modal shape $\psi(x)$.

Assume that also the vertical displacements of the cables $z_1(x, t)$ and $z_2(x, t)$ have the same longitudinal shape:

$$z_1(x, t) = Z_1(t)\ \psi(x)\ ; \qquad z_2(x, t) = Z_2(t)\psi(x) \tag{2}$$

The relative vertical displacements $\Delta y_1(x, t)$ and $\Delta y_2(x, t)$ between each cable and the corresponding point of the deck read therefore (Fig. 1)

$$\begin{aligned} \Delta y_1(x, t) &= (y + b\theta - z_1) = (Y + b\Theta - Z_1)\psi(x) = \Delta Y_1(t)\psi(x) \\ \Delta y_2(x, t) &= (y - b\theta - z_2) = (Y - b\Theta - Z_2)\psi(x) = \Delta Y_2(t)\psi(x) \end{aligned} \tag{3}$$

where $Z_i(t)$, $\Delta Y_i(t)$ denote generalised displacement components.

Assume also, as legitimate at least in the small oscillations range, that cables and deck are linear elastic around the reference (dead loads) equilibrium configuration. Then, an usual procedure of linear dynamics allows to define generalised masses and stiffnesses related to the arbitrarily chosen longitudinal shape $\psi(x)$ (e.g., Clough and Penzien 1993): it must be underlined that, differently from the "classical" sectional model in which stiffnesses and mass of the whole section are considered, each cable and the deck are considered independent from each other in the present model. Four ordinary differential equations in the four degrees of freedom $Y(t)$, $\Theta(t)$, $Z_1(t)$, $Z_2(t)$ can thus be derived.

Namely, let K_c, K_y, K_θ be the vertical (geometrical) generalised stiffness of each cable and the vertical and torsional generalised stiffness of the deck, respectively: the potential elastic energy reads

$$\Phi = \frac{1}{2}K_y Y^2 + \frac{1}{2}K_\theta \Theta^2 + \frac{1}{2}K_c(Z_1^2 + Z_2^2) + \Delta\Phi \tag{4}$$

where $\Delta\Phi$ denotes the contribution due to the deformation of the hangers, which will be discussed below (Section 3).

Denoting by m_c the generalised mass of each cable and by m_y, I the generalised mass and torsional inertia of the deck, respectively, and neglecting the mass of the hangers with respect to m_c, m_y, the kinetic energy results

$$T = \frac{1}{2}m_y \dot{Y}^2 + \frac{1}{2}I\dot{\Theta}^2 + \frac{1}{2}m_c(\dot{Z}_1^2 + \dot{Z}_2^2) \tag{5}$$

where a superimposed dot denotes derivation with respect to time t.

Note that, if all elements of the bridge oscillate with the same longitudinal shape $\psi(x)$, the motion of all sections of the bridge are similar to each other: it is this assumption that allows to describe, as proposed, the response of the whole bridge by means of a sectional model (Fig. 1), whose four degrees of freedom correspond to the generalised oscillating displacements of each bridge component $Y(t)$, $\Theta(t)$, $Z_1(t)$, $Z_2(t)$.

It might be possible to remove the assumption that the cables oscillate in the same shape as the deck: in this case, still considering few modes, the dynamics could be described by means of a pair of *global* "modes" (vertical and torsional, similar to each other as in the rigid section model), plus a pair of vertical and torsional *relative* displacement fields with a different shape (e.g., with a wave length smaller than the bridge span, as it may sometimes be appropriate); the bridge behaviour would still be described by a set of four ordinary differential equations, but the physically attractive and efficient use of a "section" model in the description of the whole dynamics is no more possible, because global and local components of displacement combine differently along the span. This alternative approach will not be explored further in this paper.

3. Small amplitude oscillations (linear behaviour of the hangers)

In the assumed reference configuration (equilibrium under dead loads) the hangers are in tension because of the weight of the deck. Therefore, as long as the relative oscillations between main cables and deck are smaller than the elongation Δy_0 corresponding to the dead weight, the hangers remain in tension (Fig. 2), and their contribution $\Delta\Phi$ to the potential elastic energy is

$$\Delta\Phi = \frac{1}{2}\int_0^L k_h \Delta y_1^2 dx + \frac{1}{2}\int_0^L k_h \Delta y_2^2 dx \tag{6}$$

where Δy_i are defined in Eq. (3) and $k_h(x)$ denotes the elastic stiffness of a row of hangers per unit length of the bridge.

Introducing Eqs. (3), Eq. (6) becomes

$$\Delta\Phi = \frac{1}{2} K_{h0} (\Delta Y_1^2 + \Delta Y_2^2) \tag{7}$$

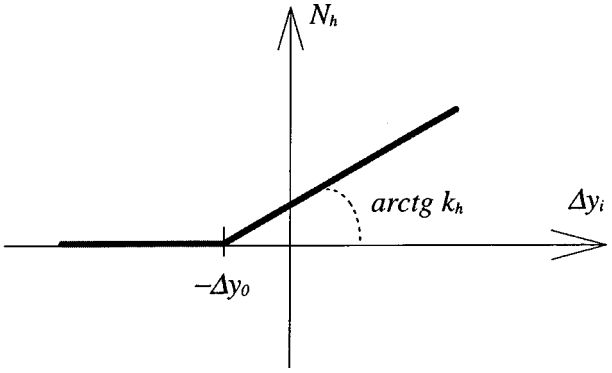

Fig. 2 Relationship between axial force N_h and relative displacement Δy_i in each hanger. Δy_i is measured from the equilibrium configuration under dead loads; Δy_0 is the static elongation due to the deck weight.

where

$$K_{h0} = \int_0^L k_h \psi(x)^2 dx \tag{8}$$

is the (elastic) generalised stiffness of one row of hangers corresponding to the assumed longitudinal shape $\psi(x)$.

The following normalisation is also introduced

$$\int_0^L \psi(x)^2 dx = L \quad \Rightarrow \quad m_c = \mu_c L, \quad m_y = \mu_y L, \quad I = i_y L \tag{9}$$

where m_c, m_y, I are the generalised masses and inertia, μ_c is the mass of each cable per unit length, and μ_y, i_y are respectively the mass and the torsional inertia of the deck per unit length (all assumed constant along the span).

If $k_h(x)$ and $\psi(x)$ are both known or given, K_{h0} can easily be obtained in closed form or by numerical integration, in analogy to K_c, K_y, K_θ.

Noting that near the ends of the main span ($x = 0$, $x = L$), displacements and torsional rotations of the deck are usually negligible, longitudinal shapes $\psi(x)$ in the form of one or more sinusoidal half waves can be acceptable approximations of pseudo-modal shapes. It can also be observed that due to the varying length of the hangers, their stiffness $k_h(x)$ is maximum at mid-span and much smaller near the ends: therefore $k_h(x)$ can also be approximated by a sinusoidal half wave.

Hence, it can be assumed :

$$\psi(x) = \sqrt{2}\sin\left(n\frac{\pi x}{L}\right), \qquad k_h(x) = k_h^{\max}\sin\frac{\pi x}{L} \tag{10}$$

with n an integer and $k_h^{\max}$ the stiffness of the shortest hangers. For $n = 1$ (no-node symmetric mode shape) and $n = 2$ (1-node anti-symmetric mode shape), Eqs. (10) yield respectively

$$n = 1 \;\Rightarrow\; K_{h0} = \frac{8}{3\pi}k_h^{\max}L \qquad n = 2 \;\Rightarrow\; K_{h0} = \frac{32}{15\pi}k_h^{\max}L \tag{11}$$

From expressions (4), (5), (7) of kinetic and elastic energy, the four Lagrange equations governing the motion are obtained

$$\begin{aligned}
&m_c\ddot{Z}_1 + 2\zeta_c\omega_c m_c\dot{Z}_1 + K_c Z_1 - K_{h0}(Y + b\Theta - Z_1) = F_{c1}(t)\\
&m_c\ddot{Z}_2 + 2\zeta_c\omega_c m_c\dot{Z}_2 + K_c Z_2 - K_{h0}(Y - b\Theta - Z_2) = F_{c2}(t)\\
&m_y\ddot{Y} + 2\zeta_y\omega_y m_y\dot{Y} + K_y Y + K_{h0}[(Y + b\Theta - Z_1) + (Y - b\Theta - Z_2)] = F_y(t)\\
&I\ddot{\Theta} + 2\zeta_\theta\omega_\theta I\dot{\Theta} + K_\theta\Theta + K_{h0}b[(Y + b\Theta - Z_1) - (Y - b\Theta - Z_2)] = M_\theta(t)
\end{aligned} \tag{12}$$

where damping terms ζ_c, ζ_y, ζ_θ have been introduced, $b = B/2$ denotes the deck half-width (Fig. 1) and angular frequencies ω_c, ω_y, ω_θ are defined as usual. Eqs. (12) include forcing terms F_{c1}, F_{c2}, F_y, M_θ on the main cables and on the deck, while no loads on the hangers have been included.

3.1. Free oscillations

A classical eigenvalue analysis of Eqs. (12) yields the four natural frequencies of the sectional model in the elastic range. Remember that Eqs. (6-8), hence Eqs. (12), hold only as long as the hangers keep taut, and also that m_c, m_y, I and K_c, K_y, K_θ represent respectively the generalised masses and stiffnesses of cables and deck considered as if they were independent from each other, while the link between them is described through K_{h0}.

For typical geometrical and mechanical parameters of long span suspension bridges, $K_y \ll K_c$, $K_\theta \ll K_c b^2$, $K_{h0} \gg K_c$ (cf. Section 4 below). Therefore, the first two modes (Fig. 3a, 3b) of free oscillation of the 4-d-o-f sectional model correspond to motions with small (often practically negligible) deformations of the hangers, and therefore their frequencies ω_1, ω_2 are almost independent from the stiffness of the hangers K_{h0} and very close to the frequencies of the classical rigid section model ($K_{h0} \to \infty$): these modes are denoted in the following as *global* vertical and torsional modes. On the other hand, the frequencies ω_3, ω_4 that correspond to *relative* modes (i.e., oscillations with cables and deck moving vertically out of phase, Fig. 3c, 3d), are much higher than the first two frequencies and are strongly influenced by K_{h0}.

3.2. Forced oscillations: limit of linear behaviour of hangers

In the case of forced oscillations, the limits of validity of Eqs. (12), i.e., of linear behaviour, are certainly of interest. Although the model can take into account loading both on the main cables and on the deck, only the weight (of deck and cables) and harmonic vertical forces on the cables are considered in the following. This load condition enhances high frequency relative motions, complementary to slow global motions well described through the rigid section model (and mainly due to actions on the deck). As already noted (and as confirmed in Section 4.1), ω_3 and ω_4 are usually much larger than ω_1, ω_2 and therefore, as long as the oscillations are small, the contributions to the dynamic response of relative and global motions, excited by forces of different nature and frequency on cables and deck, respectively, can be considered with sufficient approximation as independent from each other.

The forces on the cables are assumed vertical and harmonically varying with time (a physical justification of such actions will be discussed later, Section 4.3). The amplitude F_C and the frequency Ω of the actions are equal for both cables, with a phase lag $\Delta\varphi$ between them, that will be seen to have a great effect on the response (Appendix).

As already repeatedly stated, in the reference configuration (static equilibrium under dead loads) the hangers are in tension (Fig. 2), and thus remain as long as their relative end displacements are smaller than the corresponding elastic elongation. Otherwise, the relative oscillations may become

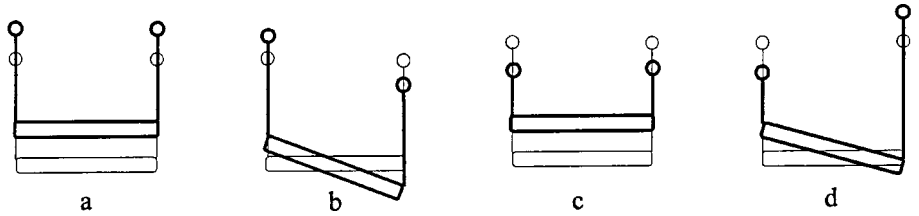

Fig. 3 Diagram of the linear modes of the 4-d-o-f sectional model

large, with hangers alternatively slack and taut.

For given damping coefficients ζ_c, ζ_y, ζ_θ and phase lag $\Delta\varphi$, the amplitude of the relative elastic oscillations depends on the action amplitude F_C and frequency Ω. If ΔY_1 and ΔY_2 are respectively the generalised relative displacement of the two rows of hangers (Eq. 3), and ΔY_0 the corresponding elastic elongation of the hangers due to the weight of the deck, in the plane of the parameters F_C, Ω the region below the lines given by the conditions

$$\max \Delta Y_1(t) = \Delta Y_0 \;\; ; \quad \max \Delta Y_2(t) = \Delta Y_0 \tag{13}$$

corresponds to small-amplitude oscillations, starting from the equilibrium configuration. An example of such boundary will be presented and discussed in Section 4.2.

Since the model is highly sensitive to selected loading frequencies, the assumed harmonic action could also be interpreted as representative of the effective component of more complex loading histories, both on the cables and on the deck or of high frequency periodic motion of main cables acted on by random large buffeting forces, as suggested by Lazer and McKenna (1990).

4. An application

An example of application of the proposed model has been developed introducing the data of the Akashi-Kaikyo suspension bridge (Katsuchi 1997), partially re-elaborated and completed by deduction when necessary (Table 1). The normalisation of Eq. (9) has also been introduced.

4.1. Free linear oscillations

Calculations and experiments have shown (Katsuchi 1997) that the longitudinal shape of the first vertical and torsional modes are symmetric and do not have nodes along the main span; therefore half-sine waves have been assumed for the modes of oscillations and for the variation of the hanger stiffness along the bridge span $k_h(x)$, according to (Eq. 10).

With values in Table 1, the linear natural frequencies of the four modes *a*, *b*, *c*, *d* of the sectional model (Fig. 3) are:

$$\omega_1 = 0.44 \;\; ; \quad \omega_2 = 0.90 \;\; ; \quad \omega_3 = 70 \;\; ; \quad \omega_4 = 170 \;\; \text{(rad/s)} \tag{14}$$

Table 1 Data and properties of the Akashi-Kaykio bridge

	mass per unit length	stiffness per unit length	modal mass for the first symmetric mode	modal stiffness for the first symmetric mode
main cable	$\mu_c = 7 \cdot 10^3$ kg/m		$m_c = 1.393 \cdot 10^7$ kg	$K_c = 8 \cdot 10^3$ KN/m
deck (vertical)	$\mu_y = 2.9 \cdot 10^4$ kg/m		$m_y = 5.771 \cdot 10^7$ kg	$K_y = 0.8 \cdot 10^3$ KN/m
deck (torsional)	$i_y = 7 \cdot 10^5$ kgm^2/m		$I = 1.393 \cdot 10^9$ kgm^2	$K_\theta = 3.2 \cdot 10^6$ KNm
hangers		$k_h^{\max} = 3 \cdot 10^4$ kN/m^2 (cf. Eq. $(10)_2$)		$K_h = 5.07 \cdot 10^7$ kN/m (Eq. $(11)_1$)
main span length $L = 1990$ m ; deck width $B = 2b = 35.5$ m. $\omega_1 = 0.44$ rad/s (1st vertical mode); $\omega_2 = 0.90$ rad/s (1st torsional mode)				

(elaborated from Katsuchi 1997)

As expected, the frequencies of the global modes *a*, *b* (ω_1, ω_2 respectively) are much smaller than the frequencies of the relative modes *c*, *d* (i.e., ω_3, ω_4).

4.2. Limit of linear behaviour

The curves (F_C, Ω) corresponding to Eq. (13) for the assumed bridge data and several phase lags $\Delta\varphi$ have been obtained as described in Appendix. Modal quantities are shown in Table 2; the results of example calculations are shown in Fig. 4 and Fig. 5, where the non-dimensional load parameter $f_c = F_C / m_C g$ has been introduced. These curves are characterised by hollows when $\Omega \approx \omega_i$, with $f_c = 0$ in the case of zero damping (Fig. 4).

The value $\Delta\varphi = 0$ represents in-phase actions on the cables, that only excite vertical motions (global and relative), without torsional motions of the deck. In this case, in the high frequency range, where the contribution of the global modes to the length variation of the hangers is negligible, the limit curve ($\Delta\varphi = 0$ in Fig. 4b) is similar to the curve found by Doole and Hogan (1996) for an 1-d-o-f piece-wise elastic system (cf. Section 5 and Fig. 6). Similarly, $\Delta\varphi = \pi$ represents actions in opposition of phase, and only the (global and relative) torsional modes develop.

For $\Delta\varphi$ different from 0 and π, both vertical and torsional modes are excited; the limit curves calculated for sample phase-lags ($\Delta\varphi = \pi/8$ and $\Delta\varphi = \pi/2$, Fig. 4a,b) and zero damping show four hollows as expected, but are always above at least one of the curves valid for $\Delta\varphi = 0$ or $\Delta\varphi = \pi$. It can be in fact demonstrated (Appendix) that for zero damping the limit condition for arbitrary $\Delta\varphi$ is given by the lower F_C value corresponding either to $\Delta\varphi = 0$ or $\Delta\varphi = \pi$ (Fig. 5a). The limit condition

Table 2 Modal quantities for the example in Section 4 (cf. Table 1 and Appendix). Eigenvectors normalised as in Eq.A7

mode	1	2	3	4
components of eigen-vectors (Eq. A7)	$A = 1.000105$	$B = 0.0563343$	$C = -0.4830409$	$D = -0.35502333$
modal mass	$m_1 = 6.14\, m_c$	$m_2 = 2.32\, m_c$	$m_3 = 2.96\, m_c$	$m_4 = 14.6\, m_c$
modal stiffness	$K_1 = 2.10\, K_c$	$K_2 = 3.27\, K_c$	$K_3 = 2.75 \cdot 10^4\, K_c$	$K_4 = 6.66 \cdot 10^5\, K_c$
modal frequency [rad/s]	$\omega_1 = 0.44$	$\omega_2 = 0.90$	$\omega_3 = 70$	$\omega_4 = 170$

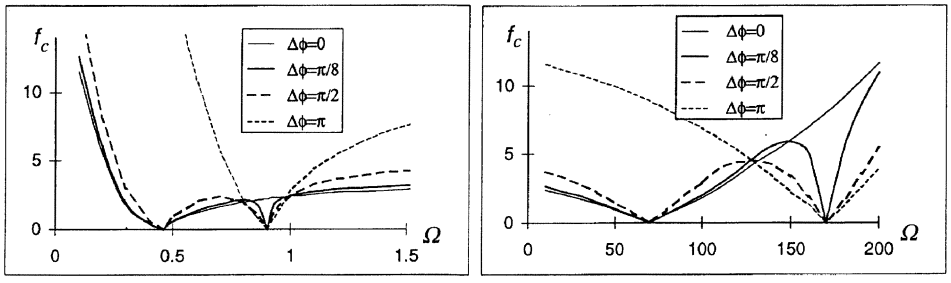

Fig. 4 Non-dimensional loading amplitude $f_c = F_C / m_C g$ *vs.* angular frequency Ω [rad/s] corresponding to upper limit of elastic behaviour, Eq. (13), for several phase lags $\Delta\varphi$ and zero damping ($m_C g$ = cable weight); a) low frequencies, b) high frequencies. The calculations refer to the values in Table 1.

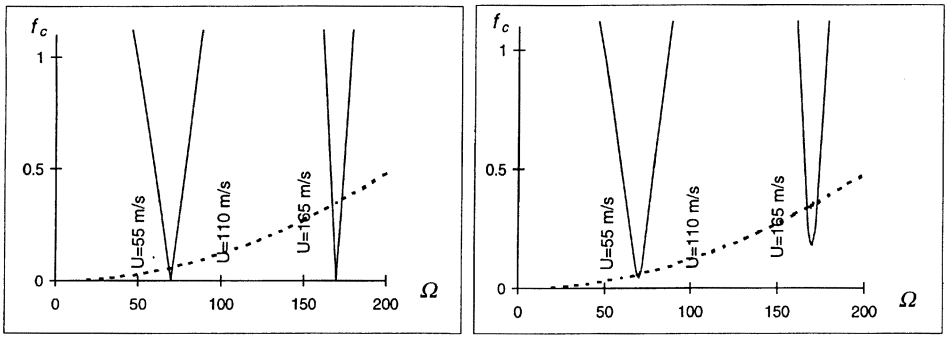

Fig. 5 Comparison of vortex shedding action with linear limit condition. Solid line: detail of limit condition for arbitrary $\Delta\varphi$ in the high frequency range: a) zero damping (cf. Fig. 4b); b) modal damping 0.5% of critical. Dashed line: values of $f_c = F_C / m_C g$ and Ω [rad/s] related to the control parameter U (mean wind speed) through the vortex shedding model (Simiu and Scanlan 1996) Eq. (15), for D = 1.4 m. Calculations made using other parameters from Table 1

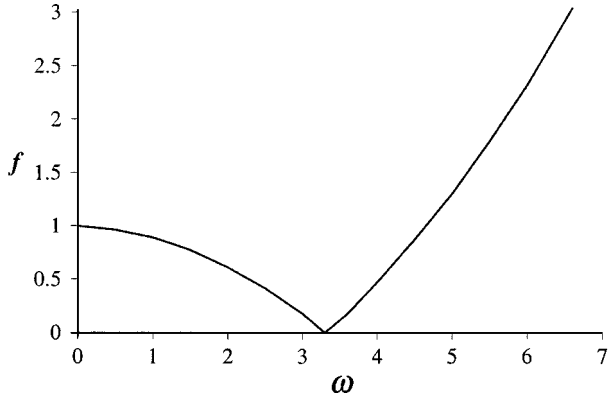

Fig. 6 Eq. (24), upper limit curve of small oscillations in the plane (f, ω) of the forcing parameters, according to Doole and Hogan (1996); f and ω are the amplitude and the frequency of the force acting on the deck, respectively.

for arbitrary phase-lag calculated in the same way with non-zero damping does not reach down the horizontal axis. A detail of this curve for $\zeta_1 = \zeta_2 = \zeta_3 = \zeta_4 = 0.005$ (i.e., damping 0.5 % of critical) is shown in Fig. 5b.

4.3. Actions due to vortex shedding

The vertical harmonic action on the cables introduced in previous Sections can be related to a widely accepted - although simplified - model of vortex shedding (Simiu and Scanlan 1996), with forcing amplitude F_C and frequency Ω both depending on a single control parameter (the mean wind speed U) through the relations

$$F_C = \frac{1}{2}\rho U^2 D C_L \sin\Omega t, \qquad \Omega = 2\pi S\frac{U}{D} \tag{15}$$

where $\rho \cong 1.25\ \mathrm{kg/m^3}$ is the air density, C_L an aerodynamic coefficient, D the cable diameter, and S the so-called "Strouhal number". C_L and S depend on the section (for a circular cylinder in appropriate range of Reynold's number: $C_L = 0.7$, $S = 0.2$).

Fig. 5a and Fig. 5b show (dashed line) the curve obtained introducing in Eqs. (15) an approximate value $D = 1.4$ m for the main cable diameter. It appears that this curve overcomes the linear limit curve, albeit in short ranges of frequencies, and with little damping: it thus appears that, with the numerical values introduced (cf. Appendix), nonlinear response can be expected for wind speed fairly high, but not unrealistic.

5. Large amplitude oscillations (unilateral behaviour of hangers)

In general, the effective generalised stiffness K_{hi} ($i = 1,2$) of the i-th row of hangers depends on the relative motion between main cables and deck. In fact, K_{hi} is equal to K_{h0}, Eq. (8), only as long as all the hangers remain in tension, hence behave elastically.

If for some hangers the relative end displacement is negative and larger than the elastic elongation due to the deck weight, the actual tangent stiffness K_{hi} becomes smaller: it varies during the oscillation, and at any instant is not larger than the elastic value K_{h0}. In fact, the larger is the oscillation amplitude, the smaller is the number of hangers that remain taut during the whole oscillation, hence the smaller is K_{hi} (softening behaviour). Assuming that all longitudinal shapes remain $\psi(x)$, K_{hi} can be expressed at any t as

$$K_{hi}(t) = \int_0^L k_h(x)\,\psi(x)^2 dx - \int_{l_i(t)} k_h(x)\,\psi(x)^2 dx = \delta_i(t) K_{h0} \qquad i = 1, 2, \tag{16}$$

where $l_i = l_i(t)$ denotes the length of the bridge where the hangers are slack (zero stiffness) at the instant t and stiffness-reduction coefficients $\delta_i(t)$, varying during the motion, are defined as

$$\delta_i(t) = K_{hi}(t) / K_{h0} \qquad 0 \le \delta_i(t) \le 1 \tag{17}$$

Thus, while each hanger has a unilateral, discontinuous stiffness, the overall stiffness of the whole row varies with continuity (assuming, of course, that the hangers are "smeared" along the span). Indeed, when a part of the hangers go slack, the shape of the bridge oscillations is likely to change during the motion. However, $\psi(x)$ in Eq. (8) is only a plausible shape compatible with the given constraints (and not a modal shape); hence a motion-dependent pseudo-modal stiffness K_{hi}, Eq. (16), can still be accepted as an approximation.

In this case, due to the time-dependence of K_{hi}, the equations governing the motion become nonlinear, and their solution could be found only by step-by-step numerical integration in the time domain. In such a way the dynamic response of the bridge could be followed for the whole range of behaviour of the hangers, but it is easy to expect that this approach would lead to very lengthy and cumbersome computations.

Augusti *et al.* (1997) introduced the simplifying and limit assumption that the stiffness-reduction coefficients δ_i can be only either 0 or 1, depending on sign and value of the generalised relative displacement introduced in Eq. (3), ΔY_i ($i = 1,2$), i.e.,

$$\delta_i = 1, \quad \text{if} \quad \Delta Y_i \ge -\Delta Y_0\ ; \qquad \delta_i = 0, \quad \text{if} \quad \Delta Y_i < -\Delta Y_0\ ; \qquad i = 1, 2, \tag{18}$$

where ΔY_0 is the already defined generalised relative displacement corresponding to the elastic

elongation of the hangers due to the weight of the deck (cf. also Eq. 13).

The assumption (18) leads to piecewise-linear equations of motion

$$
\begin{aligned}
&m_c\ddot{Z}_1 + 2\zeta_c\omega_c m_c\dot{Z}_1 + K_c Z_1 - \delta_1 K_{h0}\,(Y + b\Theta - Z_1) + (1-\delta_1)K_{h0}\Delta Y_0 = F_{c1}(t)\\
&m_c\ddot{Z}_2 + 2\zeta_c\omega_c m_c\dot{Z}_2 + K_c Z_2 - \delta_2 K_{h0}\,(Y - b\Theta - Z_2) + (1-\delta_2)K_{h0}\Delta Y_0 = F_{c2}(t)\\
&m_y\ddot{Y} + 2\zeta_y\omega_y m_y\dot{Y} + K_y Y + K_{h0}[\delta_1(Y + b\Theta - Z_1) - (1-\delta_1)\Delta Y_0 + \delta_2\,(Y - b\Theta - Z_2) - (1-\delta_2)\Delta Y_0] = F_y(t)\\
&I\ddot{\Theta} + 2\zeta_\theta\omega_\theta I\dot{\Theta} + K_\theta\Theta + K_{h0}b[\delta_1(Y + b\Theta - Z_1) - (1-\delta_1)\Delta Y_0 - \delta_2\,(Y - b\Theta - Z_2) + (1-\delta_2)\Delta Y_0] = M_\theta(t)
\end{aligned}
\tag{19}
$$

that, introducing non-dimensional variables and parameters (cf. Fig. 1)

$$
q_1 = \frac{Z_1}{b}\ , \quad q_2 = \frac{Z_2}{b}\ , \quad q_3 = \frac{Y}{b}\ , \quad q_4 = \Theta\ , \quad d_0 = \frac{\Delta Y_0}{b} \tag{20}
$$

$$
f_1 = \frac{F_{c1}}{m_c g}\ , \quad f_2 = \frac{F_{c2}}{m_c g}\ , \quad f_3 = \frac{F_y}{m_y g}\ , \quad f_4 = \frac{M_\theta b}{Ig} \tag{21}
$$

$$
\alpha = \frac{m_c}{m_y}\ , \quad \beta = \frac{m_c b^2}{I}\ , \quad \omega_h^2 = \frac{K_h}{m_c} \tag{22}
$$

become eventually

$$
\begin{aligned}
&\ddot{q}_1 + 2\zeta_c\omega_c\dot{q}_1 + \omega_c^2 q_1 - \delta_1\omega_h^2(q_3 + q_4 - q_1) + (1-\delta_1)\omega_h^2 d_0 = \frac{g}{b}f_1(t)\\
&\ddot{q}_2 + 2\zeta_c\omega_c\dot{q}_2 + \omega_c^2 q_2 - \delta_2\omega_h^2(q_3 - q_4 - q_2) + (1-\delta_2)\omega_h^2 d_0 = \frac{g}{b}f_2(t)\\
&\ddot{q}_3 + 2\zeta_y\omega_y\dot{q}_3 + \omega_y^2 q_3 +\\
&\quad + \alpha\omega_h^2[\delta_1(q_3 + q_4 - q_1) - (1-\delta_1)d_0 + \delta_2(q_3 - q_4 - q_2) - (1-\delta_2)d_0] = \frac{g}{b}f_3(t)\\
&\ddot{q}_4 + 2\zeta_\theta\omega_\theta\dot{q}_4 + \omega_\theta^2 q_4 +\\
&\quad + \beta\omega_h^2[\delta_1(q_3 + q_4 - q_1) - (1-\delta_1)d_0 - \delta_2(q_3 - q_4 - q_2) + (1-\delta_2)d_0] = \frac{g}{b}f_4(t)
\end{aligned}
\tag{23}
$$

The assumption of discontinuity in the stiffness of the cable-to-deck connections, Eq. (18), that would seem trivial if the section model shown in Fig. 1 were considered in isolation, represents only a limit hypothesis when the section model is used to describe the dynamics of the whole bridge: in fact, it would imply that all hangers suddenly pass from elastic tensile behaviour to slacking. Therefore, as already noted in Augusti *et al.* (1997), assumption (18) can be accepted as a good approximation only for large relative oscillations of the bridge in a longitudinal no-node shape, in which case most hangers of a row go slack for long intervals.

In any case, even if the vertical and torsional displacements change sign along the span, the relative stiffness K_{hi} (as defined in Eq. 16) does decrease with increasing oscillations amplitude (softening behaviour): therefore assumption (18), and consequently Eq. (19) or (23), can always be considered as a correct limit approximation of the actual behaviour.

An assumption similar to Eq. (18) has been introduced, as already said, by McKenna and his co-workers (Glover *et al.* 1989), that assumed a no-node modal shape to obtain a piecewise- linear 1-d-o-f

model from their previous model of a one-dimensional beam suspended by unilateral elastic hangers to the main cables (McKenna and Walter 1987). Instead, a progressive softening nonlinearity due to hangers behaviour has been found by Brownjohn (1994) by means of a FEM approach.

Even with assumption (18), the nonlinear dynamic response can be sought only by numerical integration of Eq. (19). A detailed investigation of nonlinear behaviour for wind-induced forces on the main cables (both in-phase and out-of-phase) and on the deck will be reported in Part II of this paper (Sepe and Augusti 2001). Due to the asymmetric behaviour of the hangers, the relative displacements between main cables and deck during the large amplitude oscillations are not symmetric with respect to the reference configuration: negative relative displacements (slack hangers: cables and deck "getting closer") are in fact much larger than relative displacements in the opposite direction, and for small structural damping can be as much as 50 times the static elongation ΔY_0 due to the dead load.

Preliminary results (Augusti *et al.* 1997), obtained for in-phase forcing on the main cables ($\Delta\varphi = 0$), showed the coexistence of multiple solutions with the same period but different amplitude and velocity for a wide range of forcing frequency below the significant linear natural frequency, as typical for softening systems.

These results show interesting analogies with results (not known to the authors at the time of writing the 1997 paper) obtained by Doole and Hogan (1996) for a 1-d-o-f system representing, as in Glover *et al.* (1989), the no-node vertical oscillations of a unidimensional beam suspended by unilateral hangers to fixed constraints. The vertical displacements y of the beam, measured from the stress free configuration, are described by the nondimensional equations

$$\begin{aligned} \ddot{y} + 2\zeta\dot{y} + (k+1)y &= g + f\ \sin\omega\tau\ , \qquad y > 0 \\ \ddot{y} + 2\zeta\dot{y} + y &= g + f\ \sin\omega\tau\ , \qquad y \le 0 \end{aligned} \tag{24}$$

where beam mass and stiffness are normalised to unity and ζ denotes the damping coefficient; g , f, ω, k represent respectively normalised beam weight, amplitude and frequency of the action on the deck and hanger stiffness.

Doole and Hogan derive analytically and numerically an upper bound of linear behaviour, i.e., a lower bound of the region of possible large amplitude oscillations (Fig. 6): this curve can be considered as the 1-d-o-f equivalent of the analogous limit curve for $\Delta\varphi = 0$ of the proposed 4-d-o-f model (Fig. 4b). Then, by means of a theoretical analysis and numerical investigation, they examine in detail the case $k = 10$, $f / g = 0.5$, and show the existence of harmonic and subharmonic steady-state response, depending on the forcing frequency; in particular, they find the coexistence of large amplitude multiple solutions, with the same period of the actions, for forcing frequencies between $\omega_a \approx 1.6$ and $\omega_b \approx 3.3$; when $\omega \approx 1.6$, the relative displacements are up to 25 times the static elastic elongation of the hangers produced by a force with intensity f. Although Doole and Hogan do not relate these significant values of the frequencies to any mechanical characteristic of the system, it seems to the writers noteworthy that ω_b corresponds almost perfectly to the natural frequency of linear oscillations $\omega_0 = \sqrt{1 + k} \approx 3.3$.

With this observation, the results by Doole and Hogan appear analogous not only to Fig. 4b in this paper, but also to the quoted preliminary numerical investigation in the nonlinear range (Augusti *et al.* 1997). In particular, they confirm the existence of large amplitude oscillations, due to nonlinear behaviour of hangers, for forcing frequencies below the significant natural elastic frequency.

6. Conclusions

The proposed 4-d-o-f model extends the classical 2-d-o-f rigid section model, drawing the attention on the possibility of relative displacements and rotations between deck and cables of suspension bridges.

Masses, stiffnesses and natural frequencies of the model are identified with appropriate generalised quantities corresponding to an assumed longitudinal shape for vertical and torsional oscillations of main cables and deck. The oscillations around the reference configuration started by vortex-shedding-like actions on the main cables can be sought by ordinary differential equations. Outside the range of small oscillations these equations become nonlinear due to the unilateral behaviour of hangers; in fact, when during the motion some or all the hangers of a row become slack, the corresponding generalised stiffness is reduced by coefficients $\delta_i \leq 1$, that depend on the sign and magnitude of the relative displacements between main cables and deck (So far, it has been assumed that either $\delta_i = 1$ or $\delta_i = 0$). No other source of nonlinearity is introduced in the model. Throughout the treatment, in fact, the restraints on the cables and the deck have been assumed linear: hence no "geometrical nonlinearity" is considered during the oscillations.

Due to the unilateral response of the hangers, the negative displacements between main cables and deck (hanger ends "getting closer") can become very large, especially in case of small structural damping. A wide investigation in the nonlinear range of response will be presented in a following paper: preliminary results always indicate the coexistence of multiple solutions with the same period but different amplitude and velocity for a wide range of forcing frequency below the significant linear natural frequencies, as typical for softening systems.

The proposed simple model is just an intermediate step to describe wind-induced relative motions between main cables and deck and could be further refined. For example, a first improvement might be to attribute to the stiffness reduction coefficient δ_i (by means of numerical techniques) values in the whole range between 0 and 1, depending on how many hangers are slack.

Along a similar line, the model could also be extended to describe the local motion of a part of the bridge, taking into account, for example, higher vibration modes of the cables, with frequencies in between those of the pseudo-modal shapes here considered, depending on the wave length. In such cases the displacements of the cables, in addition to the mechanism of large amplitude oscillations already discussed, could reach significant amplitude also as a consequence of lock-in with vortex shedding forces.

The model could also allow to evaluate the wind induced oscillations (buffeting) in the sub-critical range of wind speed, i.e., far from self-excited or resonant oscillations. Also of interest are the relative oscillations due to the different nature and intensity of the wind actions on the main cables and the deck, which for very long span bridges are significantly distant from each other.

However, the main goal of the proposed model was only to identify qualitatively unusual phenomena that might be experienced by suspension bridges much longer than existing ones. From the analytical developments and the preliminary calculations presented, it would appear that large relative translations and rotations between cables and deck, allowed by the unilateral behaviour of the hangers, cannot be excluded to occur under plausible wind speeds and can perhaps explain some phenomena observed in the Tacoma and Golden Gate bridges.

These results seem already sufficient to warn designers not to limit *a priori* their considerations to phenomena already observed and studied for existing bridges. The actual possibility and significance of other phenomena, like those indicated in the present paper, can come only from detailed

calculations and specific experimental research.

Acknowledgements

This paper has been prepared within two National Research Projects on Wind Engineering (RESACIV and ACME-CUE) partially supported by the Italian Ministry for University and Research (MURST). The authors thank the Referees for their suggestions, that allowed to improve the paper.

References

Ahmed N.U. and Harbi H. (1998), "Mathematical analysis of dynamic models of suspension bridges", *SIAM J. Appl. Math.*, **58**(3), 853-874.

Augusti G., Sepe V. and Della Vedova M. (1997), "A nonlinear model for the analysis of wind-induced oscillations of suspension bridges", *Proc. 2nd Euro-African Conference on Wind Engineerin*g, Genoa, 22-26 June, **2**, 1617-1624.

Augusti G. and Sepe V. (1999), "A deformable section model of large suspension bridges: the limit condition for linear response", *Proceedings of the Fourth European Conference on Structural Dynamics EURODYN '99*, Prague, June 1999, **2**, 771-776.

Brownjohn J.M.W. (1994), "Observations on nonlinear dynamic characteristics of suspension bridges", *Earthquake Engineering and Structural Dynamics*, **23**, 1351-1367.

Clough R.W. and Penzien J. (1993), *Dynamics of Structures*, McGraw-Hill, 2nd Edition.

D'Asdia P. and Sepe V. (1998), "Aeroelastic instability of long span suspended bridges: a multi-mode approach", *Journal of Wind Engineering and Industrial Aerodynamics*, **74-76**, 849-857.

Doole S.H. and Hogan S.J. (1996), "A piecewise linear suspension bridge model: nonlinear dynamics and orbit continuation", *Dynamic and Stability of Systems*, **11**, 19-47.

Ewins D.J. (1984), *Modal testing: theory and practice*, Research Studies Press LTD. - J. Wiley & Sons.

Glover J., Lazer A.C. and McKenna P.J. (1989), "Existence and stability of large scale nonlinear oscillations in suspension bridges", *Journ. of Applied Mathematics and Physics (ZAMP)*, **40**, 172-200.

Jain A., Jones N.P. and Scanlan R.H. (1996), "Coupled aeroelastic and aerodynamic response analysis of long-span bridges", *Journal of Wind Engineering and Industrial Aerodynamics*, **60**, 69-80.

Katsuchi H. (1997), "An analytical study on flutter and buffeting of the Akashi-Kaikyo Bridge", *MSc Thesis*, The Johns Hopkins University, Baltimore (USA).

Lazer, A.C. and McKenna P.J. (1990), "Large-amplitude periodic oscillations in suspension bridges: some new connections with nonlinear analysis", *SIAM Review*, **32**(4), 537-578.

McKenna, P.J. and Walter W. (1987), "Nonlinear oscillation in a suspension bridge", *Archive of Rational Mechanics and Analysis*, **98**, 167-177.

Sepe V. and Augusti G. (2001), "A "deformable section" model for the dynamics of suspension bridges. Part II: Large amplitude oscillations", [*in preparation*].

Simiu E. and Scanlan R.H. (1996). *Wind Effects on Structures*, J. Wiley & Sons, 3rd Edition.

Appendix: Calculation of the limit curve of linear response (Fig. 4-5)

Denote by $\underline{q}$ the vector of Lagrangian coordinates

$$\underline{q}(t) = \begin{bmatrix} Z_1(t) \\ Z_2(t) \\ Y(t) \\ \Theta(t) \end{bmatrix}. \tag{A1}$$

The linear dynamics of the system (small oscillations around the configuration of equilibrium under dead loads) is governed by the Eqs. (12), now rewritten as

$$\underline{\underline{M}}\,\ddot{\underline{q}} + \underline{\underline{C}}\,\dot{\underline{q}} + \underline{\underline{K}}\,\underline{q} = \underline{f}(t) \tag{A2}$$

where

$$\underline{\underline{M}} = \begin{bmatrix} m_c & 0 & 0 & 0 \\ 0 & m_c & 0 & 0 \\ 0 & 0 & m_y & 0 \\ 0 & 0 & 0 & I \end{bmatrix}, \quad \underline{\underline{K}} = \begin{bmatrix} K_c + K_{h0} & 0 & -K_{h0} & -bK_{h0} \\ 0 & K_c + K_{h0} & -K_{h0} & bK_{h0} \\ -K_{h0} & -K_{h0} & 2K_{h0} + K_y & 0 \\ -bK_{h0} & bK_{h0} & 0 & K_\theta + 2b^2K_{h0} \end{bmatrix}$$

$$\underline{\underline{C}} = \begin{bmatrix} 2\zeta_c\omega_c m_c & 0 & 0 & 0 \\ 0 & 2\zeta_c\omega_c m_c & 0 & 0 \\ 0 & 0 & 2\zeta_y\omega_y m_y & 0 \\ 0 & 0 & 0 & 2\zeta_\theta\omega_\theta I \end{bmatrix} \tag{A3}$$

The assumed external actions consist of harmonic vertical forces on the cables, with intensity F_C equal for both cables and phase-lag $\Delta\varphi$; the force vector can therefore been expressed as

$$\underline{f}(t) = \frac{1}{2}\underline{f}_0 \exp(i\Omega t) + c.c. = \frac{1}{2}\begin{bmatrix} F_C \\ F_C\exp(i\Delta\varphi) \\ 0 \\ 0 \end{bmatrix}\exp(i\Omega t) + c.c. = \begin{bmatrix} F_C\cos\Omega t \\ F_C\cos(\Omega t + \Delta\varphi) \\ 0 \\ 0 \end{bmatrix} \tag{A4}$$

where *c.c.* denotes the complex conjugate vector, $i^2 = -1$, Ω is the angular frequency of the forcing, and the meaning of the other symbols is easily deduced from the equation itself.

As a consequence, the linear steady-state response of the system can be written as

$$\underline{q}(t) = \frac{1}{2}\underline{q}_0 \exp(i\Omega t) + c.c. \tag{A5}$$

Indicating by $\underline{\underline{\Psi}}$ the matrix of the eigenvectors $\underline{\psi}_r$ of the dynamic problem and by K_r the stiffness of the rth mode of the sectional model, the complex amplitude $\underline{q}_0$ is (Ewins 1984)

$$\underline{q}_0 = \sum_{r=1}^{4} \frac{1}{K_r} \frac{\underline{\psi}_r^T \underline{f}_0}{\left(1 - \left(\frac{\Omega}{\omega_r}\right)^2\right) + i\left(2\zeta_r\frac{\Omega}{\omega_r}\right)} \underline{\psi}_r \tag{A6}$$

Due to the symmetry of the problem, $\underline{\underline{\Psi}}$ can also be represented and normalised as

$$\underline{\underline{\Psi}} = [\,\underline{\psi}_1 \;\; \underline{\psi}_2 \;\; \underline{\psi}_3 \;\; \underline{\psi}_4\,] = \begin{bmatrix} 1 & 1 & 1 & 1 \\ 1 & -1 & 1 & -1 \\ A & 0 & C & 0 \\ 0 & B & 0 & D \end{bmatrix}; \tag{A7}$$

therefore, denoting by ΔY_0 the static change of length of the hangers due to the deck weight and by $\Delta Y_{1(0)}$, $\Delta Y_{2(0)}$, the amplitudes of the relative oscillations during the motion, it results also:

$$G_0 = \frac{\Delta Y_0}{m_c g} = \frac{m_y}{m_c(2K_{h0} + K_y)} \tag{A8}$$

$$G_1(\Omega, \Delta\varphi) = \frac{\Delta Y_{1(0)}}{F_c} =$$

$$= \frac{1}{K_1}\frac{\left(1-\left(\frac{\Omega}{\omega_1}\right)^2\right)(1+\cos\Delta\varphi) + 2\zeta_1\frac{\Omega}{\omega_1}\sin\Delta\varphi}{\left(1-\left(\frac{\Omega}{\omega_1}\right)^2\right)^2 + \left(2\zeta_1\frac{\Omega}{\omega_1}\right)^2}(A-1) + \frac{1}{K_2}\frac{\left(1-\left(\frac{\Omega}{\omega_2}\right)^2\right)(1-\cos\Delta\varphi) - 2\zeta_2\frac{\Omega}{\omega_2}\sin\Delta\varphi}{\left(1-\left(\frac{\Omega}{\omega_2}\right)^2\right)^2 + \left(2\zeta_2\frac{\Omega}{\omega_2}\right)^2}(Bb-1) +$$

$$+\frac{1}{K_3}\frac{\left(1-\left(\frac{\Omega}{\omega_3}\right)^2\right)(1+\cos\Delta\varphi) + 2\zeta_3\frac{\Omega}{\omega_3}\sin\Delta\varphi}{\left(1-\left(\frac{\Omega}{\omega_3}\right)^2\right)^2 + \left(2\zeta_3\frac{\Omega}{\omega_3}\right)^2}(C-1) + \frac{1}{K_4}\frac{\left(1-\left(\frac{\Omega}{\omega_4}\right)^2\right)(1-\cos\Delta\varphi) - 2\zeta_4\frac{\Omega}{\omega_4}\sin\Delta\varphi}{\left(1-\left(\frac{\Omega}{\omega_4}\right)^2\right)^2 + \left(2\zeta_4\frac{\Omega}{\omega_4}\right)^2}(Db-1)$$

$$G_2(\Omega, \Delta\varphi) = \frac{\Delta Y_{2(0)}}{F_c} =$$

$$= \frac{1}{K_1}\frac{\left(1-\left(\frac{\Omega}{\omega_1}\right)^2\right)(1+\cos\Delta\varphi) + 2\zeta_1\frac{\Omega}{\omega_1}\sin\Delta\varphi}{\left(1-\left(\frac{\Omega}{\omega_1}\right)^2\right)^2 + \left(2\zeta_1\frac{\Omega}{\omega_1}\right)^2}(A-1) - \frac{1}{K_2}\frac{\left(1-\left(\frac{\Omega}{\omega_2}\right)^2\right)(1-\cos\Delta\varphi) - 2\zeta_2\frac{\Omega}{\omega_2}\sin\Delta\varphi}{\left(1-\left(\frac{\Omega}{\omega_2}\right)^2\right)^2 + \left(2\zeta_2\frac{\Omega}{\omega_2}\right)^2}(Bb-1) +$$

$$+\frac{1}{K_3}\frac{\left(1-\left(\frac{\Omega}{\omega_3}\right)^2\right)(1+\cos\Delta\varphi) + 2\zeta_3\frac{\Omega}{\omega_3}\sin\Delta\varphi}{\left(1-\left(\frac{\Omega}{\omega_3}\right)^2\right)^2 + \left(2\zeta_3\frac{\Omega}{\omega_3}\right)^2}(C-1) - \frac{1}{K_4}\frac{\left(1-\left(\frac{\Omega}{\omega_4}\right)^2\right)(1-\cos\Delta\varphi) - 2\zeta_4\frac{\Omega}{\omega_4}\sin\Delta\varphi}{\left(1-\left(\frac{\Omega}{\omega_4}\right)^2\right)^2 + \left(2\zeta_4\frac{\Omega}{\omega_4}\right)^2}(Db-1) \tag{A9}$$

Peaks in $G_1(\Omega, \Delta\varphi)$ and $G_2(\Omega, \Delta\varphi)$ exist when Ω is close to one of the natural frequencies ω_i.

Introducing the non-dimensional amplitude $f_C = F_C/(m_C g)$ (cf. Eq. (21)), the condition defining the linear range

$$|\Delta Y_{1(0)}| \le \Delta Y_0 \quad ; \quad |\Delta Y_{2(0)}| \le \Delta Y_0 \tag{A10}$$

becomes

$$f_C \le \frac{G_0}{|G_1(\Omega, \Delta\varphi)|} \quad ; \quad f_C \le \frac{G_0}{|G_2(\Omega, \Delta\varphi)|} \tag{A11}$$

Consequently, the limit curves $f_C(\Omega, \Delta\varphi)$ are

$$f_C(\Omega, \Delta\varphi) = \min\left\{\frac{G_0}{|G_1(\Omega, \Delta\varphi)|} \ , \ \frac{G_0}{|G_2(\Omega, \Delta\varphi)|}\right\}. \tag{A12}$$

They are characterised by hollows when $\Omega \approx \omega_i$ (Fig. 4, 5), corresponding to $f_C = 0$ in the limit case of zero damping.

The curves in Fig. 4 and Fig. 5 are obtained with the numerical values introduced in Sec.4 (cf. Table 1), that lead to the modal quantities shown in Table 2.

In particular, Fig. 4 and Fig. 5a report limit curves for the case of zero damping. The limit curve for $\Delta\varphi = 0$ represents actions on the cables perfectly in phase, that excite only the global and relative vertical motions, with no torsion of the deck; similarly, the limit curve for $\Delta\varphi = \pi$ represents actions perfectly out of phase, that excite only the global torsional and the relative torsional modes.

It is evident from Fig. 4 that the other two cases considered ($\Delta\varphi = \pi/8$, $\Delta\varphi = \pi/2$) yield limit curves above

either the curve for $\Delta\varphi = 0$ or the curve for $\Delta\varphi = \pi$. This is valid in general in absence of mechanical damping; in this case, in fact, it results (cf. Eq. A8, A9)

$$\frac{\Delta Y_{1(0)}}{F_c} = Q(1 + \cos\Delta\varphi) + R(1 - \cos\Delta\varphi) \quad , \quad \frac{\Delta Y_{2(0)}}{F_c} = Q(1 + \cos\Delta\varphi) - R(1 - \cos\Delta\varphi) \tag{A13}$$

with

$$Q = \frac{A - 1}{K_1[1 - (\Omega/\omega_1)^2]} + \frac{C - 1}{K_3[1 - (\Omega/\omega_3)^2]} \quad , \quad R = \frac{bB - 1}{K_2[1 - (\Omega/\omega_2)^2]} + \frac{bD - 1}{K_4[1 - (\Omega/\omega_4)^2]} \tag{A14}$$

and also

$$\Delta\varphi = 0 \Rightarrow \frac{\Delta Y_{1(0)}}{F_C} = \frac{\Delta Y_{2(0)}}{F_C} = 2Q \ , \ \Delta\varphi = \pi \Rightarrow \frac{\Delta Y_{1(0)}}{F_C} = -\frac{\Delta Y_{2(0)}}{F_C} = 2R . \tag{A15}$$

For a given phase-lag, therefore, the maximum relative displacements are smaller or equal to those for $\Delta\varphi = 0$ or $\Delta\varphi = \pi$ if $|R| \leq |Q|$ or $|R| \geq |Q|$, respectively; as a consequence, the limit curves $f_C(\Omega, \Delta\varphi)$ for zero damping (Eq. A12, Fig. 4 and Fig. 5a) are always bounded from below by either the curve for $\Delta\varphi = 0$ or $\Delta\varphi = \pi$, and attain the value $f_C = 0$ when $\Omega = \omega_i$.

For damping different from zero, also the ordinate of the limit curve $f_C(\Omega, \Delta\varphi)$ is different from zero for $\Omega = \omega_i$ (Fig. 5b). If the damping is small as in Fig. 5b (0.5% of critical damping, Eq. (A9)) the broken line, related to the mean wind speed U through the vortex shedding model (Simiu and Scanlan 1996) still overcome the linear range for $\Omega \cong \omega_3$ or $\Omega \cong \omega_4$, and in these cases therefore large amplitude oscillations can be possible. For larger values of damping, on the contrary, hollows become smoother, and the possibility of large amplitude oscillations may disappear within the range of wind speeds of technical interest.